Electronic transport in *k*-component Fibonacci quantum waveguides

2000 J. Phys.: Condens. Matter 12 5701

(http://iopscience.iop.org/0953-8984/12/26/316)

J. Phys.: Condens. Matter **12** (2000) 5701–5712. Printed in the UK PII: S0953-8984(00)12664-5

Electronic transport in k-component Fibonacci quantum waveguides

R W Peng, G J Jin, Mu Wang, A Hu, S S Jiang and D Feng

National Laboratory of Solid State Microstructures, Nanjing University, Nanjing 210093, China
and
Centre for Advanced Studies in Science and Technology of Microstructures, Nanjing 210093, China

Received 16 March 2000

Abstract. We present a study of electronic behaviours in the k-component Fibonacci (KCF) quantum waveguides, in which k different incommensurate intervals are arranged according to a substitution rule. On the basis of the transfer matrix method, the quantum transmission properties of the KCF stub structures are obtained. It is shown that the transmission coefficient depends on the wavevector of the electron and the number of different incommensurate intervals k. For the KCF waveguides with the same k, on increasing the number of stubs, the minima in transmission extend gradually into the band gap over which the transmission is blocked. Meanwhile more transmission peaks appear. For finite KCF stub structures, on increasing the number of different incommensurate intervals k, the total transmission over the spectral region of interest decreases gradually and the width of the electronic band gap is enlarged. Moreover, when the value of k is large enough, the transmission is basically shut off, except at a few energies where resonant tunnelling takes place. These properties make it possible to use this kind of KCF waveguide as a switching device for digital applications. On the other hand, the charge-density distributions in these structures are singularly continuous. We propose that they can be analysed using a multifractal concept. A dimensional spectrum of singularities associated with the charge density, $f(\alpha)$, demonstrates that the electronic transport in the KCF waveguide presents scaling properties; hence the charge-density distribution shows a genuine multifractality.

1. Introduction

Recently considerable interest has been shown in mesoscopic systems [1–14], in which electron transport is governed by quantum mechanics rather than classical electrodynamics. Due to the fact that the characteristic size in a mesoscopic system is smaller than the phase coherence length of an electron, and of the same order as the de Broglie wavelength, quantization of the transverse motion becomes an important issue. A variety of interesting interference phenomena have been exhibited, such as the quantized conductance in point contacts, persistent currents in metallic loops, universal conductance fluctuation, and Coulomb blockade, which has opened up a completely new branch of device physics and mesoscopic physics [12]. In particular, the electron motion is ballistic or quasiballistic at low temperatures, the electronic transport is identical to the microwave propagation through a waveguide, and the allowed modes in these structures are considered to be waveguide modes. Considering a quantum analogue of well-known microwave or optical devices, these electronic properties of the mesoscopic systems may have potential applications in quantum interference devices [5, 15, 16].

In the past decade, several studies [6–14] have been reported on one-dimensional (1D) quantum waveguide structures, such as a T-shape device consisting of a main wire attached to

0953-8984/00/265701+12$30.00

a stub perpendicular to the wire. It has been proposed theoretically [6, 7] that a semiconductor stub structure exhibits a transistor function. In particular, for the case of one-channel T-shape structures, the transmission oscillates between zero and one, and results similar to those for waveguides resonantly coupled to a cavity have been achieved [8, 9]. On the other hand, the waveguide characteristics of electron transport through a wide–narrow–wide structure have also been observed in experiments by the splitting-gate technique [17, 18]. More recently, Xia [19] proposed a simple 1D waveguide theory for a quantum wire with one or two stubs. Singha Deo and Jayannavar [12] extended it to a multiple-serial-stub structure and demonstrated how a single defect in a periodic system modifies the band properties nontrivially. In addition, the electron waveguide with side-branch structures also shows some novel transmission characteristics [13]. Now that the electron behaviours in quantum waveguides are known to depend critically upon the geometric structure, it is interesting to investigate the electron transport in quantum waveguides with various configurations, such as periodic, quasiperiodic, and even other aperiodic structures.

One of the well-known examples in one-dimensional (1D) quasiperiodic systems is the Fibonacci sequence. The Fibonacci sequence can be produced by repeating the substitution rules $A \to AB$ and $B \to A$, in which the ratio of the numbers of the two incommensurate intervals A and B is equal to the golden mean $\tau = (\sqrt{5}+1)/2$. Since Merlin *et al* reported the first realization of Fibonacci superlattices [20], much attention has been paid to the exotic wave phenomena of Fibonacci systems in x-ray scattering spectra [20–22], Raman scattering spectra [23, 24], optical transmission spectra [25–28], and in propagation modes of acoustic waves on corrugated surfaces [29, 30]. However, only a few studies [14] have been devoted to the electronic transport through quasiperiodic quantum waveguides. To the best of our knowledge, there seems to have been no work on the quantum waveguide with 1D aperiodic structure which contains more than two incommensurate intervals, although its structural character and other physical properties have become known [31–35].

In this paper, we present the electronic transport in serial-stub waveguides arranged in k-component Fibonacci (KCF) sequences, which contain k incommensurate intervals A_i ($i = 1, 2, \ldots, k$) and can be generated by the substitution rules

$$\begin{aligned} A_1 &\to A_1 A_k \\ A_k &\to A_{k-1} \\ &\vdots \\ A_i &\to A_{i-1} \\ &\vdots \\ A_2 &\to A_1. \end{aligned}$$

With a transfer matrix method, the electronic transport through the KCF quantum waveguides is calculated. For KCF quantum waveguides with the same k, on increasing the number of stubs, the minima in transmission become extended gradually into band gaps over which the transmission is blocked. Meanwhile, more transmission peaks appear. For a series of finite KCF waveguides, on increasing the number of different incommensurate intervals k, the total transmission over the spectral region of interest decreases gradually and the width of the electronic band gap (transmission zero) is enlarged. On the other hand, the charge-density distributions in these structures are singularly continuous and are analysed using a multifractal concept. It is known that multifractal analysis is a suitable statistical description of the long-term dynamical behaviour of a physical system [36, 37]. The multifractal formalism relies on the nonuniformity of the system. Generally for 'strongly' disordered

systems with exponentially decaying correlations, the wavefunctions themselves manifest multifractal properties [38, 39]; Fibonacci chains represent in a sense 'weakly' disordered systems. Our investigation demonstrates that in the KCF quantum waveguides, the charge-density distributions present scaling properties of multifractality, too.

2. The theoretical model

The k-component Fibonacci structures (KCFS) are defined as follows. Consider the substitution S acting on an alphabet of k elements $A_1, A_2, \ldots, A_i, \ldots, A_k$ according to the following rule:

$$S\begin{pmatrix} A_1 \to A_1A_k \\ A_k \to A_{k-1} \\ \vdots \\ A_i \to A_{i-1} \\ \vdots \\ A_2 \to A_1 \end{pmatrix}.$$

Thereafter, these k elements are arranged in a KCF sequence. For example, the three-component Fibonacci structure ($k = 3$) consists of three kinds of element A_1, A_2, and A_3. On the basis of the substitution rules S: $A_1 \to A_1A_3$, $A_3 \to A_2$, and $A_2 \to A_1$, these three kinds of element are sequenced as $A_1A_3A_2A_1A_1A_3A_1A_3A_2\cdots$. On the other hand, the KCFS can also be described as a limit of the generations of the sequence $C_n^{(k)}$. Let $C_n^{(k)} = S^nA_1$; thus

$$\begin{aligned} C_0^{(k)} &= A_1 \\ C_1^{(k)} &= A_1A_k \\ C_2^{(k)} &= A_1A_kA_{k-1} \\ &\vdots \\ C_{k-1}^{(k)} &= A_1A_kA_{k-1}\cdots A_3A_2 \end{aligned}$$

and in general

$$C_n^{(k)} = C_{n-1}^{(k)} + C_{n-k}^{(k)} \qquad (\text{if } n > k).$$

Define the number of elements in the generation $C_n^{(k)}$ as $F_n^{(k)}$. It follows that $F_n^{(k)}$ satisfies $F_n^{(k)} = F_{n-1}^{(k)} + F_{n-k}^{(k)}$ with $F_i = i + 1$ ($i = 0, 1, \ldots, k-1$). We denote the number of A_i ($i = 1, 2, \ldots, k$) in $C_n^{(k)}$ as $N_n^{(k)}(A_i)$. The ratios of these numbers are defined as

$$\eta_i = \lim_{n\to\infty}[N_n^{(k)}(A_i)/N_n^{(k)}(A_1)].$$

It turns out that the set $\{\eta_i\}$ satisfies

$$\begin{aligned} &\eta_k^k + \eta_k = 1 \\ &1{:}\eta_k = \eta_k{:}\eta_{k-1} = \cdots = \eta_i{:}\eta_{i-1} = \cdots = \eta_3{:}\eta_2. \end{aligned} \tag{1}$$

Therefore all of these ratios $\eta_i = \eta_k^{k-i+1}$ ($1 < i \leqslant k$) are irrational numbers between zero and unity except $\eta_1 = 1$. It has been proven [31] that the KCFS are quasiperiodic when $1 < k \leqslant 5$; while for $k > 5$, the KCFS are nonquasiperiodic, but they are still ordered.

The system that we study here is that of the k-component Fibonacci (KCF) quantum waveguides, where the quantum wire is attached by a series of stubs perpendicular to it (as shown in figure 1). The model of the KCFS with elements $A_1, A_2, \ldots, A_i, \ldots, A_k$ is associated

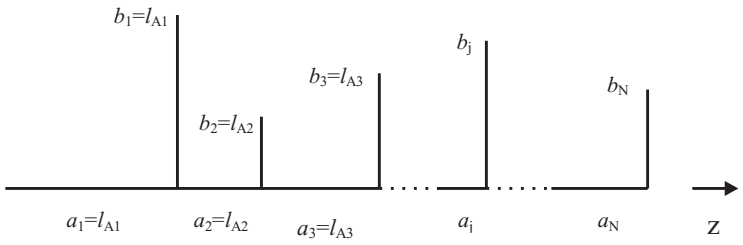

Figure 1. A schematic KCF stub structure. a_j and b_j are the lengths of the jth wire segment and the jth stub, respectively. These lengths a_j and b_j are arranged according to the KCF sequence $C_n^{(k)}$. For example, if $k = 3$, i.e., in the 3CF stub structure, there are three kinds of length l_{A_1}, l_{A_2}, and l_{A_3}, which are arranged as $A_1A_3A_2A_1A_1A_3A_1\cdots$. Thereafter, the lengths of the stubs will successively be $b_1 = l_{A_1}, b_2 = l_{A_3}, b_3 = l_{A_2}, b_4 = l_{A_1}, \ldots$. And the situation is similar for the wire segments.

with k kinds of real length $l_{A_1}, l_{A_2}, \ldots, l_{A_k}$. We suppose that in the KCF waveguides, both the wire segments and the stubs consist of these k lengths $(l_{A_1}, l_{A_2}, \ldots, l_{A_k})$. In the wire segments, the lengths are chosen successively according to the KCF sequence, and the same is true of the stubs. Let the wire segments with stubs be labelled sequentially with positive integer j from left to right, while a_j and b_j are the lengths of the jth wire segment and the jth stub, respectively (shown in figure 1). For example, if $k = 3$, i.e., in the 3CF waveguide, there should be three different lengths $l_{A_1}, l_{A_2}, l_{A_3}$ which are arranged as the 3CF sequence $(A_1A_3A_2A_1A_1A_3A_1A_3A_2\cdots)$. Thereafter, the lengths of stubs will successively be $b_1 = l_{A_1}$, $b_2 = l_{A_3}, b_3 = l_{A_2}, b_4 = l_{A_1}, b_5 = l_{A_1}, \ldots$. And there are similar situations for the wire segments $(a_1 = l_{A_1}, a_2 = l_{A_3}, a_3 = l_{A_2}, a_4 = l_{A_1}, \ldots)$. Now consider electron transport in the KCF waveguides. We assume that the width of the structure is narrow enough compared to the length of the structure. It follows that the system can be regarded as quasi-one-dimensional and retains quantum interference. In any segment or stub, an electron is free-particle-like. When the electron with energy $\epsilon = \hbar^2q^2/2m$ (where q is the wavevector) is injected from one side, it can pass through the structure ballistically provided that the continuum conditions are satisfied.

Suppose that the electronic wavefunctions in the jth segment and jth stub are plane-wave-like: $\psi_j(z) = g_j \exp(\mathrm{i}qz) + h_j \exp(-\mathrm{i}qz)$ and $\varphi_j(z) = u_j \exp(\mathrm{i}qz) + v_j \exp(-\mathrm{i}qz)$, respectively. A local coordinate is chosen for each segment and stub. For the segment, its origin is positioned at the left-hand side of the segment; while for each stub, the origin is positioned at the lower end of the stub. The upper end of each stub in figure 1 is assumed to be rigid under the external gate voltage. Using the Griffiths boundary condition at the intersections, the electronic amplitudes in the $(j+1)$th segment can be obtained from those in the jth segment as follows [14]:

$$\begin{pmatrix} g_{j+1} \\ h_{j+1} \end{pmatrix} = S_{j+1,j} \begin{pmatrix} g_j \\ h_j \end{pmatrix}. \tag{2}$$

The transfer matrix $S_{j+1,j}$ has the form

$$S_{j+1,j} = \begin{pmatrix} 1 - \dfrac{\mathrm{i}}{2}\cot(qb_j) & -\dfrac{\mathrm{i}}{2}\cot(qb_j) \\ \dfrac{\mathrm{i}}{2}\cot(qb_j) & 1 + \dfrac{\mathrm{i}}{2}\cot(qb_j) \end{pmatrix} \begin{pmatrix} \mathrm{e}^{\mathrm{i}qa_j} & 0 \\ 0 & \mathrm{e}^{-\mathrm{i}qa_j} \end{pmatrix} \tag{3}$$

where a_j and b_j are the lengths of the wire segment and stub, respectively. In order to get a transfer matrix with components that are real functions, the amplitudes are transformed as

follows:

$$\begin{pmatrix} g_j \\ h_j \end{pmatrix} = \begin{pmatrix} 1 & \mathrm{i} \\ 1 & -\mathrm{i} \end{pmatrix} \begin{pmatrix} \alpha_j \\ \beta_j \end{pmatrix}. \tag{4}$$

Thereafter, $S_{j+1,j}$ is transformed into $T_{j+1,j}$ for a new set of amplitudes (α_j, β_j), which satisfies

$$\begin{pmatrix} \alpha_{j+1} \\ \beta_{j+1} \end{pmatrix} = T_{j+1,j} \begin{pmatrix} \alpha_j \\ \beta_j \end{pmatrix} \tag{5}$$

and the new transfer matrix $T_{j+1,j}$ can be written as

$$T_{j+1,j} = \begin{pmatrix} 1 & 0 \\ -\cot(qb_j) & 1 \end{pmatrix} \begin{pmatrix} \cos(qa_j) & -\sin(qa_j) \\ \sin(qa_j) & \cos(qa_j) \end{pmatrix}. \tag{6}$$

If the lengths of all segments and stubs and the initial values of the amplitudes (α_1, β_1) are known, the amplitudes along the quantum wire can be obtained recursively from

$$\begin{pmatrix} \alpha_{j+1} \\ \beta_{j+1} \end{pmatrix} = M(j) \begin{pmatrix} \alpha_1 \\ \beta_1 \end{pmatrix} \tag{7}$$

where

$$M(j) = \prod_{i=1}^{j} T_{i+1,i}.$$

For the KCF waveguides in which the lengths of segments and stubs are ordered as the generation $C_n^{(k)}$, the corresponding transfer matrix takes the form

$$M_n^{(k)} = M_{n-k}^{(k)} M_{n-1}^{(k)} \tag{8}$$

where

$$\begin{aligned} M_0^{(k)} &= T_1^{(k)} = I \\ M_1^{(k)} &= T_{k,1}^{(k)} T_1^{(k)} \\ M_2^{(k)} &= T_{k-1,k}^{(k)} T_{k,1}^{(k)} T_1^{(k)} \\ &\vdots \\ M_{k-1}^{(k)} &= T_{2,3}^{(k)} T_{3,4}^{(k)} \cdots T_{k-1,k}^{(k)} T_{k,1}^{(k)} T_1^{(k)}. \end{aligned}$$

Therefore many important quantities in the KCF waveguides can be readily derived from equations (6)–(8). From the global transfer matrix $M_n^{(k)} = M$, the reflection amplitude and the transmission coefficient can be written as [40]

$$R[C_n^{(k)}] = -\frac{1}{2 + \mathrm{Tr}(M^* M)} [(M_{11}^2 - M_{12}^2 + M_{21}^2 - M_{22}^2) - 2\mathrm{i}(M_{11} M_{12} + M_{21} M_{22})] \tag{9}$$

and

$$T[C_n^{(k)}] = \frac{4}{\mathrm{Tr}(M^* M) + 2} \tag{10}$$

respectively. M_{11}, M_{12}, M_{21}, and M_{22} are the four elements of $M_n^{(k)} = M$. On the other hand, the charge density in the jth segment of the waveguides is determined by

$$\begin{aligned} \left|\psi_j(z)\right|^2 &= \left|A_j \mathrm{e}^{-\mathrm{i}qz} + B_j \mathrm{e}^{-\mathrm{i}qz}\right|^2 \\ &= 4\left|\alpha_j\right|^2 \cos^2(qz) + 4\left|\beta_j\right|^2 \sin^2(qz) - 2(\alpha_j^* \beta_j + \alpha_j \beta_j^*) \sin(2qz) \end{aligned} \tag{11}$$

In fact, the incident electron of the system is described by $\mathrm{e}^{\mathrm{i}qz}$; thus the initial amplitudes are $\alpha_1 = (1 + R)/2$ and $\beta_1 = (1 - R)/2\mathrm{i}$. The system becomes deterministic; therefore, the electron transport through the KCF quantum waveguide is determined by equations (8)–(11).

3. Electronic transmission spectra for the KCF waveguides

On the basis of equations (8)–(11), the electron transmission through the KCF waveguides can be calculated. As we mentioned in section 2, in the KCF stub waveguide, k different lengths $l_{A_1}, l_{A_2}, \ldots, l_{A_k}$ are arranged in both the wire segments and the stubs according to the KCF sequence $C_n^{(k)}$ (as shown in figure 1). We consider the simplest setting to illustrate the physical effect of the geometrical structures. Choose $l_{A_1} = 1$ and $l_{A_i} = \eta_i$ $(i = 2, 3, \ldots, k)$, where η_i can be given by equation (1).

A series of electron transmission spectra of the KCF waveguides have been studied by increasing the number of stubs and by varying the number of incommensurate intervals k. As an example, figure 2 gives the transmission coefficient T as a function of the wavevector q in the interval $(0, \pi]$ for the three-component Fibonacci waveguides ($k = 3$) with the generations $C_7^{(3)}$, $C_9^{(3)}$, $C_{11}^{(3)}$, $C_{13}^{(3)}$. The three different intervals $\{A_i\}$ $(i = 1, 2, 3)$ are $l_{A_1} = 1$, $l_{A_2} = 0.465\,571$, $l_{A_3} = 0.682\,328$, respectively. It is clear that in the case of a very small number of stubs, there is no total reflection, although there exist some regions of minimum transmission. When the number of stubs becomes large, the minima in transmission become extended gradually into the band gap where the transmission is blocked. Generally, on increasing the number of stubs in the waveguide, more and more transmission zones diminish

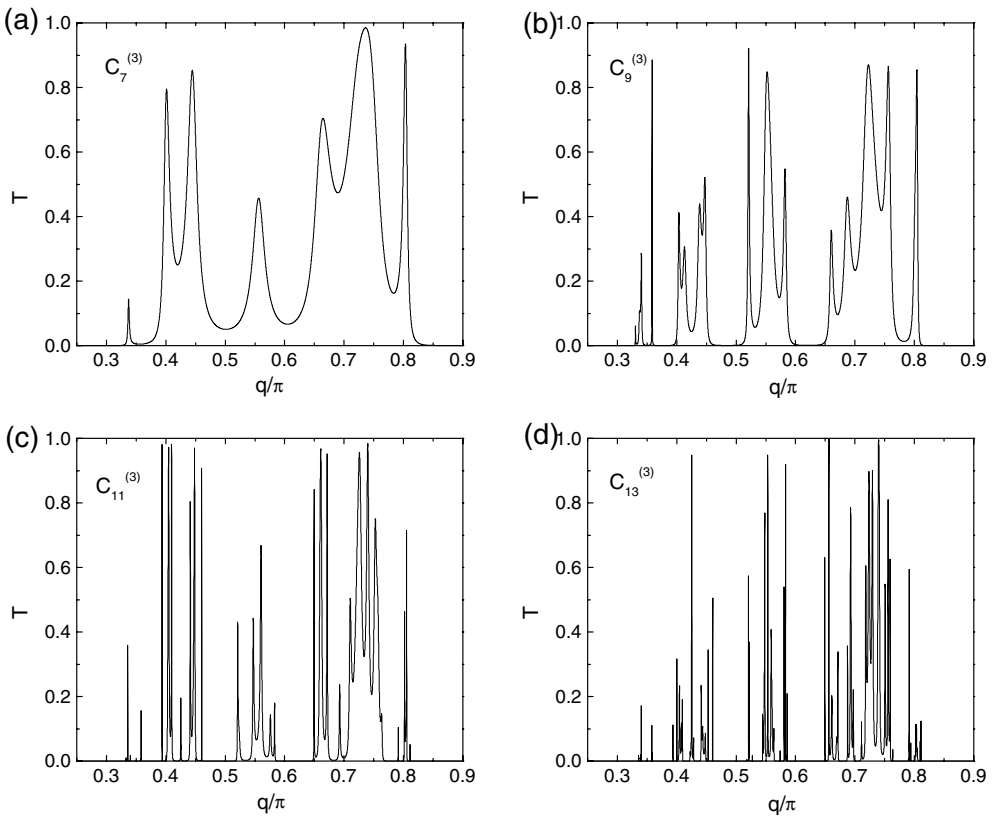

Figure 2. The transmission coefficient T as a function of the wavevector q for the three-component Fibonacci structures with the following generations and numbers of stubs: (a) $C_7^{(3)}$ and $N = 13$; (b) $C_9^{(3)}$ and $N = 28$; (c) $C_{11}^{(3)}$ and $N = 60$; (d) $C_{13}^{(3)}$ and $N = 129$.

gradually, and some of them approach zero transmission. In this way, a one-dimensional electronic band gap is realized. To explain this feature quantitatively, we define an 'average transmission' as

$$\langle T\rangle_{ave} = \frac{1}{\pi}\int_0^{\pi} T(q)\,\mathrm{d}q. \tag{12}$$

It follows that the 'average transmissions' of figures 2(a)–2(d) are $\langle T\rangle_{ave} \cong 0.153$, 0.0875, 0.0467, 0.0216, respectively. Therefore the total transmission over the spectral region of interest definitely decreases when the number of stubs in the KCF waveguides (k is fixed) increases due to the appearance of electronic band gaps. Meanwhile, more transmission peaks emerge. Most interestingly, some transmission peaks locate in between the band gaps. This property suggests potential applications in quantum interference devices.

It is enlightening to compare the behaviours of the electron transport through KCF waveguides with different numbers of incommensurate intervals k. The calculations are performed on the transmission of different KCF waveguides with almost identical numbers of stubs. Figure 3 illustrates the transmission coefficient T as a function of the wavevector q for four KCF waveguides with different k. It can be seen that on increasing k, the band gaps are easily observed. Meanwhile the 'average transmission' defined by equation (12)

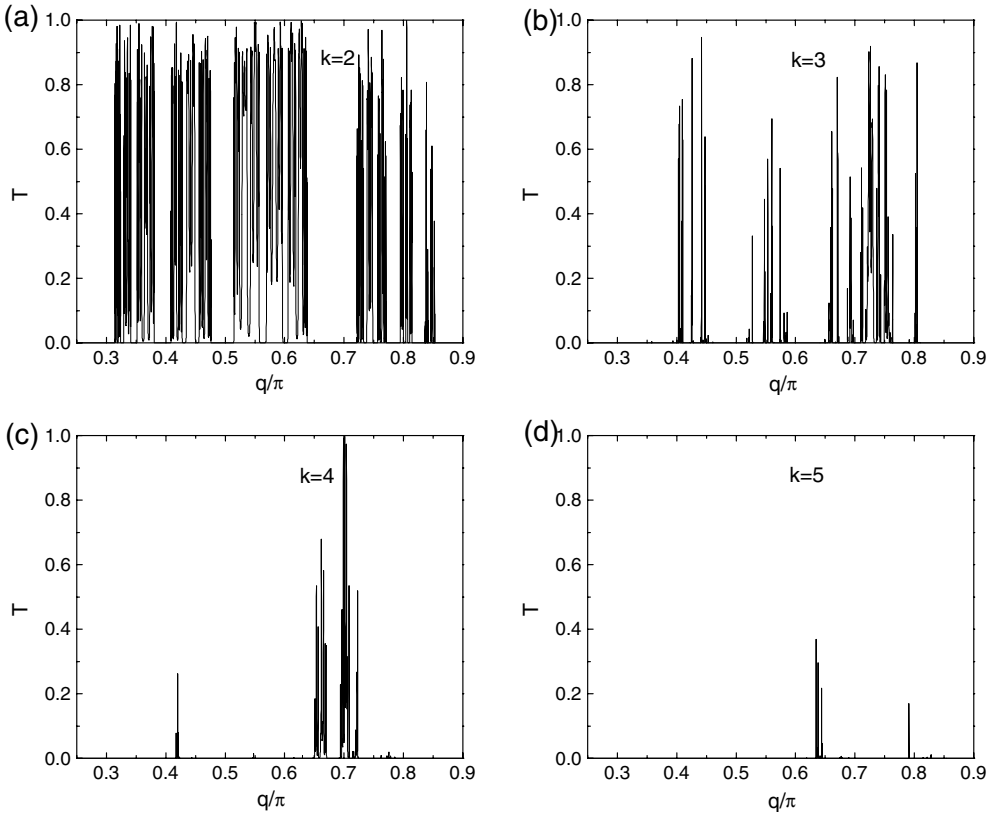

Figure 3. The transmission coefficient T as a function of the wavevector q for the k-component Fibonacci structures with different numbers of incommensurate intervals k. The values of k, the generations, and the numbers of stubs N are as follows: (a) $k = 2$, $C_{12}^{(2)}$, and $N = 233$; (b) $k = 3$, $C_{15}^{(3)}$, and $N = 277$; (c) $k = 4$, $C_{17}^{(4)}$, and $N = 250$; (d) $k = 5$, $C_{19}^{(5)}$, and $N = 245$.

varied as $\langle T\rangle_{ave} \cong 1.03 \times 10^{-1}$, 1.07×10^{-2}, 4.94×10^{-3}, and 8.17×10^{-5} corresponding to figures 3(a)–3(d), respectively. It follows that the total transmission over the spectral region decreases gradually and much wider band gaps appear when k increases in the KCF waveguides. Moreover, when the value of k is sufficiently large, the transmission is basically shut off, except at a few energies where resonant tunnelling takes place. It seems that if we consider the KCF waveguides for discrete logic applications, sufficient noise margins and sharp transitions between logic levels might be more easily achieved, due to the fact that the 'on' and 'off' states are evident enough as shown in figure 3(c) and 3(d). From this point of view, we suggest that the KCF structure might be a good candidate for use in the structural design of high-performance quantum devices for digital applications.

4. The charge-density distributions in the KCF waveguides and their scaling properties

The charge-density distributions in the KCF waveguides can be obtained from equation (11). Generally they are aperiodic and inhomogeneous. In order to compare the distributions in different KCF waveguides, we consider the charge density corresponding to the largest electronic transmission in the KCF waveguides. Figures 4(a)–4(d) illustrate the charge-density distributions with the same parameters as for figures 3(a)–3(d). For example, the charge-density distribution in figure 4(a) corresponds to the largest transmission in the 2CF waveguide ($k = 2$), where the wavevector $q = 0.805\,46\,\pi$ and the transmission coefficient $T = 0.999\,79$. It is shown that these different transmission probabilities designate statistical

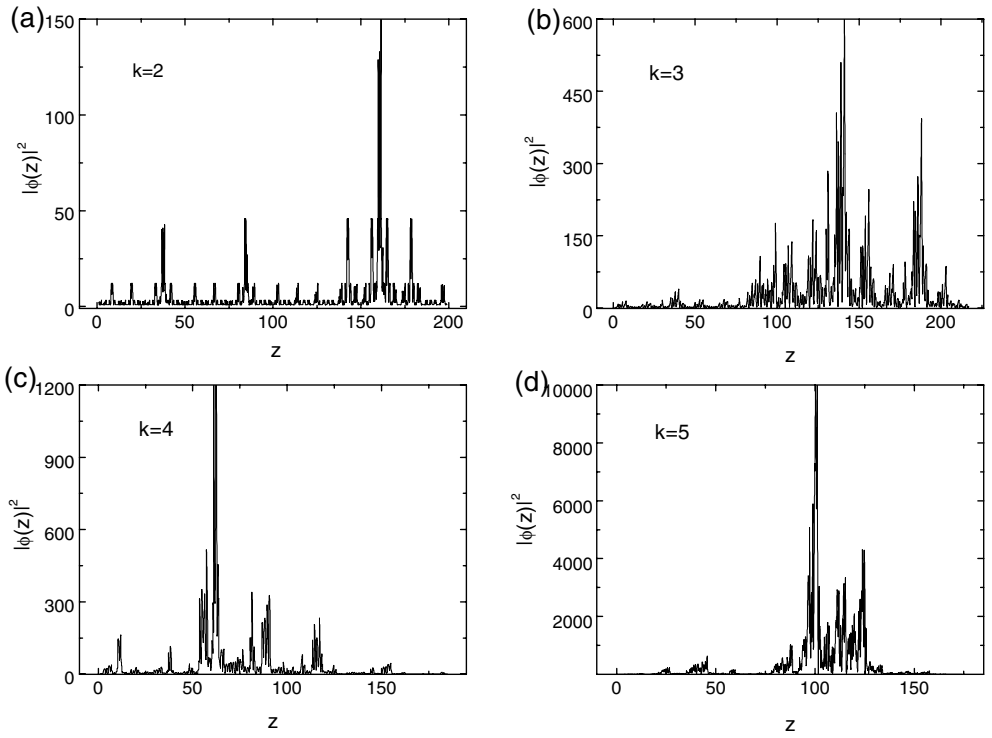

Figure 4. The charge-density distributions of the KCF waveguides with the same parameters as for figure 3. (a) $k = 2$, $q = 0.805\,46\,\pi$, $T = 0.999\,79$; (b) $k = 3$, $q = 0.404\,84\,\pi$, $T = 0.993\,95$; (c) $k = 4$, $q = 0.701\,11\,\pi$, $T = 0.999\,96$; (d) $k = 5$, $q = 0.634\,45\,\pi$, $T = 0.367\,91$.

self-similar behaviours. As k increases, the statistical behaviours change rapidly and become rather complicated (as shown in figures 4(b)–4(d)). In fact, the charge-density distributions in figure 4 are neither discrete nor absolutely continuous. These complicated spectra can be characterized by the multifractal concept.

Multifractal analysis is a tool for characterizing the nature of a positive measure in a statistical sense [41–44]. If a positive measure is expressed by boxes of size ε and the probability $p_i(\varepsilon)$ in the ith box, an exponent (singularity strength) α_i can be defined as

$$p_i(\varepsilon) \sim \varepsilon^{\alpha_i}. \tag{13}$$

If we count the number of boxes $N(\alpha)\,\mathrm{d}\alpha$ where the probability p_i has singularity strength between α and $\alpha + \mathrm{d}\alpha$, then $f(\alpha)$ can be loosely defined as the fractal dimension of the set of boxes with singularity strength α. That is

$$N(\alpha)\,\mathrm{d}\alpha \sim \varepsilon^{-f(\alpha)}\,\mathrm{d}\alpha. \tag{14}$$

The $f(\alpha)$ singularity spectrum provides a mathematically precise and intuitive description of the nonuniform system.

In the case of electronic transmission probability distributions, the charge density is a positive quantity in the space. A straightforward application of the multifractal formalism requires the evaluation of an exact integral of the measure of the structures with infinite length over a small segment of length in the space. In this case, the computer time required for the calculation will increase incredibly. To solve this problem, an approximate scheme is chosen [44]. Instead of performing calculations for the infinite KCF waveguide, we only deal with a structure which contains repeating copies of the finite generation, i.e., $C_n^{(k)}$, of the original structure. It is known that the transmission of a periodic waveguide is also periodic. Therefore we need only consider the situation in one period of space. The essential ingredient in multifractal characterization is the probability weights p_i. In our case, p_i is defined as the weight of the charge density in the density spectrum, i.e.,

$$p_i = |\psi(z_i)|^2 \Big/ \left(\sum_{i=1}^{N} |\psi(z_i)|^2 \right) \tag{15}$$

where ψ_i is the charge density (shown in equation (11)) with the position $z_i = Di/N$ $(i = 1, 2, \ldots, N)$, D is the total length of the wire segments in the KCF waveguide, and N is the number of times that the copying is performed. The partition function can then be expressed as

$$\begin{aligned} Z(Q) &= \sum_{i=1}^{N} p_i^Q \\ Z'(Q) &= \frac{\mathrm{d}Z}{\mathrm{d}Q} = \sum_{i=1}^{N} p_i^Q \ln p_i \\ Z''(Q) &= \frac{\mathrm{d}^2 Z}{\mathrm{d}^2 Q} = \sum_{i=1}^{N} p_i^Q (\ln p_i)^2 \end{aligned} \tag{16}$$

where the parameter Q provides a 'microscope' for exploring the singular measure in different regions. For $Q > 1$, $Z(Q)$ amplifies the more singular regions of p_i, while for $Q < 1$ it accentuates the less singular regions. For $Q = 1$ the measure $Z(1)$ replicates the original measure. The $f(\alpha)$ curve of any finite sample is therefore available at a local level, i.e., for a

given phase space. The values of α and $f(\alpha)$ are given by

$$\alpha = -\frac{Z'(Q)}{Z(Q)\ln N}$$
$$f(\alpha) = \frac{1}{\ln N}\left(\ln Z(Q) - \frac{QZ'(Q)}{Z(Q)}\right). \tag{17}$$

In order to illustrate the multifractality of the charge-density distributions of the KCF waveguides shown in figures 4(a)–4(d), we calculate the corresponding $f(\alpha)$ spectra (shown in figure 5) according to equations (15)–(17). In figure 5, the data points fit perfectly onto a smooth curve, which is a characteristic feature of an infinite structure. The quantity $f(\alpha)$ is the dimension of the set of positions z_i in the charge-density spectrum. In particular, we are interested in the physical meanings in the $f(\alpha)$ spectrum of a density measure:

(i) The abscissa α_0 of the summit of the $f(\alpha)$ curve, which corresponds to $Q = 0$, is the strength of a generic singularity. In some senses, the exponent α_0 characterizes the behaviour of the density at a generic singularity. Obviously $f(\alpha_0) = D_0 = 1$, which means that the support of the density is the whole z-axis.

(ii) For $Q = 1$, $f(\alpha(1)) = \alpha(1) = D_1$; D_1 is the information dimension of the density measure:

$$D_1 = \lim_{\varepsilon\to 0}\left[\left(-\sum_i p_i(\varepsilon)\ln p_i(\varepsilon)\right)\Big/(\ln(1/\varepsilon))\right]$$

where $-p_i(\varepsilon)\ln(p_i(\varepsilon))$ is an expression from information theory and corresponds to the amount of information associated with the distribution of $p_i(\varepsilon)$ values. The distance of D_1 from unity is a faithful measure of how singular the density measure is. Figure 5 shows that the information dimension D_1 in the KCFS is less than the dimension of the support D_0, i.e., $D_1 < D_0 = 1$. So the charge-density distribution of the KCF waveguides is definitely a fractal measure.

(iii) The extremes α_{min} and α_{max} of the abscissa of a $f(\alpha)$ curve represent the minimum and the maximum of the singularity exponent α which acts as an appropriate weight in phase space. In fact, α_{min} and α_{max} characterize the scaling properties of the most concentrated and most rarefied regions of the density measure respectively. On increasing of the number of incommensurate intervals k in the KCF waveguides, the value $\Delta\alpha = \alpha_{max} - \alpha_{min}$ also

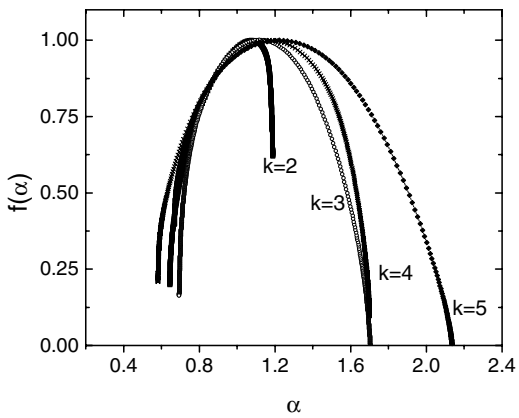

Figure 5. $f(\alpha)$ spectra for the charge-density distributions of the KCF waveguides where $k = 2$, 3, 4, 5.

increases gradually. This implies that the charge-density measure of the KCF waveguides approaches the behaviour of a random system when k increases.

(iv) The dimension of the set of transmission peaks $d_p = f(1)$, corresponding to $\alpha = 1$. d_p represents the dimension of the set of positions z for which the local singularity exponent α is less than unity. In figure 5 we have $d_p < 1$. This further confirms that the charge-density spectrum of the KCF waveguide is definitely a fractal measure.

The above scaling analysis indicates that the charge-density distributions of the KCF waveguides are singularly continuous and possess multifractality. Different KCF waveguides exhibit different electronic transport probability distributions.

5. Conclusions

We have presented the electronic transmission through k-component Fibonacci (KCF) waveguides, which contain k different incommensurate intervals and can be generated by a substitution rule. The transmission spectra have been obtained by a transfer matrix method. It has been demonstrated that the transmission coefficient has a rich structure. For the KCF waveguides with a fixed k, the electron can be localized and the band gap appears when the number of stubs becomes sufficiently large. On increasing k, the width of the electronic band gap enlarges, while for a sufficiently large k, the transmission is basically shut off, except at a few energies where resonant tunnelling takes place. These interesting features make the KCF structure a possible candidate for use in high-performance quantum devices. On the other hand, the charge-density distributions in the KCF waveguides are neither discrete nor absolutely continuous. Multifractal analysis reveals that these density measures can be characterized by a dimension spectrum of singularities $f(\alpha)$. The $f(\alpha)$ spectrum is a smooth function with a summit of $D_1 < D_0 = 1$. The charge-density measure does not have an absolutely continuous component. Therefore the electronic transport through the KCF waveguides ($2 \leqslant k \leqslant 5$) is singularly continuous and possesses multifractal properties.

Acknowledgments

This work was supported by a grant from the National Natural Science Foundation of China, the State Key Programme for Basic Research from the Ministry of Science and Technology of China, and the provincial Natural Science Foundation of Jiangsu.

References

[1] Kramer B 1991 *Quantum Coherence in Mesoscopic Systems (NATO Advanced Study Institute Series B: Physics, vol 254)* (New York: Plenum)
[2] Altshuler B L, Lee P A and Webb R A 1991 *Mesoscopic Phenomena in Solids* (Amsterdam: North-Holland)
[3] Imry Y 1997 *Introduction to Mesoscopic Physics* (New York: Oxford University Press)
[4] Washburn S and Webb R A 1986 *Adv. Phys.* **35** 375
[5] Datta S and McLennan M J 1990 *Rep. Prog. Phys.* **53** 1003
[6] Sols F, Macucci M, Ravaioli U and Hess K 1989 *Appl. Phys. Lett.* **54** 350
[7] Sols F, Macucci M, Ravaioli U and Hess K 1989 *J. Appl. Phys.* **66** 3892
[8] Porod W, Shao Z and Lent C S 1992 *Appl. Phys. Lett.* **61** 1350
[9] Porod W, Shao Z and Lent C S 1993 *Phys. Rev.* B **48** 8495
[10] Takeman E and Bagwell P F 1993 *Phys. Rev.* B **48** 2553
[11] Wu Hua, Sprung D W L, Martorell J and Klarsfeld S 1991 *Phys. Rev.* B **44** 6351
[12] Singha Deo P and Jayannavar A M 1994 *Phys. Rev.* B **50** 11 629
[13] Shi J R and Gu B Y 1997 *Phys. Rev.* B **55** 4703

[14] Jin G J, Wang Z D, Hu A and Jiang S S 1999 *J. Appl. Phys.* **85** 1597
[15] Thornton T J 1995 *Rep. Prog. Phys.* **58** 311
[16] Capasso F and Datta S 1990 *Phys. Today* **43** (2) 74
[17] Kouwenhoven L P, Hekking F W J, van Wees B J, Harmans C J P M, Timmering C E and Foxon C T 1990 *Phys. Rev. Lett.* **65** 361
[18] Katsumoto S, Sano N and Kobayashi S 1993 *Solid State Commun.* **85** 223
[19] Xia J B 1992 *Phys. Rev.* B **45** 3593
[20] Merlin R, Bajema K, Clarke R, Juang F-Y and Bhattacharya P K 1985 *Phys. Rev. Lett.* **55** 1768
[21] Todd J, Merlin R, Clarke R, Mohanty K M and Axe J D 1986 *Phys. Rev. Lett.* **57** 1157
[22] Hu A, Tien C, Li X, Wang Y and Feng D 1986 *Phys. Lett.* A **119** 313
[23] Bajema K and Merlin R 1987 *Phys. Rev.* B **36** 4555
[24] Wang C and Barrio R A 1988 *Phys. Rev. Lett.* **61** 191
[25] Kohmoto M, Sutherland B and Iguchi K 1987 *Phys. Rev. Lett.* **58** 2436
[26] Gellermann W, Kohmoto M, Sutherland B and Taylor P C 1994 *Phys. Rev. Lett.* **72** 633
[27] Riklund R and Severin M 1988 *J. Phys. C: Solid State Phys.* **21** 3217
[28] Dulea M, Severin M and Riklund R 1990 *Phys. Rev.* B **42** 3680
[29] Desideri J P, Macon L and Sornette D 1989 *Phys. Rev. Lett.* **63** 390
[30] Kono K, Nakada S, Narahara Y and Ootuka Y 1991 *J. Phys. Soc. Japan* **60** 368
[31] Hu A, Wen Z X, Jiang S S, Tong W T, Peng R W and Feng D 1993 *Phys. Rev.* B **48** 829
[32] Peng R W, Wang Mu, Hu A, Jiang S S and Feng D 1995 *Phys. Rev.* B **52** 13 310
Peng R W, Jin G J, Wang Mu, Hu A, Jiang S S and Feng D 1999 *Phys. Rev.* B **59** 3599
[33] Tong P 1995 *Phys. Rev.* B **52** 16 301
Ali M K and Gumbs G 1988 *Phys. Rev.* B **38** 7091
[34] Liu Y, Fu X, Han H, Cheng B and Luan C 1991 *Phys. Rev.* B **43** 13 240
[35] Cai M, Liu Y and Deng M 1994 *Phys. Rev.* B **49** 5429
[36] Halsey T C, Jensen M H, Kadanoff L P, Procaccia I and Shraiman B I 1986 *Phys. Rev.* A **33** 1141
[37] Meakin P, Coniglio A, Stanley H E and Witten T 1986 *Phys. Rev.* A **34** 3325
[38] Fal'ko V I and Efetov K B 1995 *Phys. Rev.* B **52** 17 413
[39] Efetov K B 1997 *Phys. Rev. Lett.* **79** 491
Efetov K B 1997 *Phys. Rev.* B **56** 9630
[40] Pichard J L and Sarma G 1981 *J. Phys. C: Solid State Phys.* **14** L127
[41] Paladin G and Vulpiani A 1987 *Phys. Rep.* **156** 147
[42] Feder J 1988 *Fractals* (New York: Plenum)
[43] Chhabra A and Jensen R V 1989 *Phys. Rev. Lett.* **62** 1327
[44] Godrèche C and Luck J M 1990 *J. Phys. A: Math. Gen.* **23** 3769